Metals and Materials International (2020) 26:1515–1523
https://doi.org/10.1007/s12540-019-00397-x

Formation of Metastable Aluminides in Al–Sc–Ti (Zr, Hf) Cast Alloys

E. Popova[1] · P. Kotenkov[1,2] · A. Shubin[1] · I. Gilev[1]

Received: 7 February 2019 / Accepted: 23 July 2019 / Published online: 7 August 2019

Abstract
The effect of the ternary alloys composition and overheating of their melts (at 100–370 K above the liquidus temperature) on the morphology and composition of aluminides in the Al–Sc–Ti, Al–Sc–Zr, Al–Sc–Hf systems were investigated. It was shown that during the crystallization of these melts under certain conditions, the primary precipitated phase are the complex aluminides $Al_3(Sc_xZr_{1-x})$, $Al_3(Sc_xTi_{1-x})$, $Al_3(Sc_xHf_{1-x})$ having a metastable cubic lattice with $L1_2$ structure, which matches the α-Al structural type. The variety of growth forms of aluminides is explained by a combination of a number of factors: the magnitude of overheating of the melt, the difference in the diffusion coefficients of transition metals, and the local concentration of transition metals in the respective growth zones.

Keywords Aluminum alloys · Transition metals · Phase formation · Aluminides · Synthesis · Thermal stability · Hot-resistant lightweight alloy · Cubic lattice

1 Introduction

The main direction of further improving the characteristics of heat-resistant aluminum alloys are the additions of transition (TM) and rare-earth metals (REM) [1–5]. Small additions of TM and REM can control the structure and dispersion hardening of aluminum and aluminum-based alloys. It becomes possible due to the formation of thermally stable dispersoids—secondary precipitates of intermetallic phases, which determine the high level of strength characteristics of these alloys [6–10]. One of the necessary conditions for achieving a high modifying effect of aluminum alloys with small additions of transition metals is the formation of TM aluminides (the nucleating phase) during crystallization, the lattices of which have a crystallographic and dimensional similarity to the α-Al lattice. Among all d-block transition elements, only scandium forms stable aluminides with a cubic $L1_2$ crystal structure, similar to the α-Al lattice [11]. With additions of scandium exceeding the eutectic composition, i.e. when Al_3Sc is formed, the maximum grinding effect of the grain in a modified alloy is achieved. Stable trialuminides formed by other elements of the periodic system, for example, Ti, Zr, Hf (the fourth group), have tetragonal *D*022 and *D*023 crystal structures, exhibiting a needle-like shape in cross-section. Only some of the crystallographic planes of these lattices coincide with the α-Al, having FCC crystal structure. Metastable trialuminides Ti, Zr, Hf with a cubic lattice are obtained by rapid crystallization of superheated Al–TM melts [12–15], when the formation of thermodynamically stable phases is suppressed due to internal stresses arising in the alloy.

Recently, special attention is paid to the development of ternary master alloys with two TMs, forming complex metastable aluminides [16, 17]. The composition of the aluminides, their growth forms, and their distribution in the alloy are determined. When modifying and alloying aluminum alloys with small additions of such master alloys, a synergistic effect of grain refinement appears [18, 19] and it becomes possible to control the alloys structure formation.

A series of ternary Al–Sc–Ti, Al–Sc–Zr, and Al–Sc–Hf master alloys were investigated; the formation conditions of metastable aluminides having different morphology and composition were studied. Under the equilibrium conditions of binary Al–Sc, Al–Ti, Al–Zr, and Al–Hf melts crystallization the eutectic transformation in the Al–Sc [20] system

✉ P. Kotenkov
p.kotenkoff@yandex.ru

[1] Laboratory of Physical Chemistry of Metallurgical Melts, Institute of Metallurgy of the Ural Branch of the Russian Academy of Sciences, 101 Amundsena street, Yekaterinburg, Russia 620016

[2] Department of Metallurgy of Iron and Alloys, Ural Federal University Named After the First President of Russia B. N. Yeltsin, 19 Mira street, Yekaterinburg, Russia 620002

occurs at 0.28 at% Sc and 660° C; peritectic transformations in systems Al–Ti, Al–Zr, Al–Hf [21, 22] occurs at 0.079 at% Ti, 0.033 at% Zr, 0.078 at% Hf and temperatures 665.4, 660.8 and 662.2 °C, respectively.

2 Materials and Experimental Procedures

In the process of ternary alloys preparation were used commercial master alloys Al–1.7Ti and Al–0.6Zr (at%), as well as Al–1.2Sc and Al–0.59Hf (at%), pre-synthesized using high-purity aluminum (99.97%), pure scandium (99.9%) and electrolytic hafnium. The melting was carried out in a furnace in graphite crucibles in an argon atmosphere, dissolving the master alloys in liquid aluminum for 30 min. A tungsten–rhenium thermocouple was used to determine the temperature of the melt. The melts were poured into a bronze mold, the size of obtained ingots was $100 \times 80 \times 10$ mm (mass of ingots was about 200 g), with the rate of the crystallization was in the range from 100 to 1000 K/s. The achieved overheating of the melts above the liquidus temperatures was estimated as follows. The chemical analysis of obtained alloys was carried out utilizing ICP optical emission spectrometer OPTIMA 2100 DV. Liquidus temperatures of ternary alloys were determined by the additive method, based on the results of chemical analysis and the state diagrams of binary systems [20–22]. Thus, the superheating values of the melts were found to be in the range from 85° to 370°.

The metallographic analysis of the samples was performed using a microscope OLYMPUS GX-57 at magnifications of 50 × to 1500 × and a scanning electron microscope Carl Zeiss EVO 40. The chemical composition of TM aluminides, matrix, α-phase dendritic cells, and eutectic precipitates were determined utilizing Energy Dispersive.

X-rays Spectrometer (EDX) Oxford Instruments INCA x-act. The composition of at least ten aluminide particles of different sizes and growth forms was determined: from white (trialuminides composition) to contrast gray (a solid solution of aluminides in α-Al, with the ratio of one TM to another was constant). Moreover, from three to five aluminide particles having different morphologies were scanned in each alloy. The all electronic images shown in this paper were obtained using a backscattered electron (BSE) detector with an atomic number contrast (Z-contrast).

The compositions of Al–Sc–Ti, Al–Sc–Zr, Al–Sc–Hf master alloys and metastable aluminides formed in them (stable in some cases) are displayed in Table 1. The values

Table 1 The main characteristics of the Al–Sc–TM experimental alloys (TM: Ti, Zr, Hf)

No	The alloys composition and ΣTM, at%; lattices parameter of α-Al, nm	ΔT, K	TM/Sc		The aluminides composition, lattice types, max. size, μm	The lattices parameter, the lattice mismatch with α-Al, %	
			In alloys	In aluminides		Calculated	Experimental
1	Al–0.60Sc–0.07Ti ΣTM = 0.67 0.40462(10) nm	215	0.12	0.14	Al3($Sc_{0.88}Ti_{0.12}$) $L1_2$ up to 3–4 μm	0.4087 nm 1%	0.40746(10) nm 0.7%
2	Al–0.56Sc–0.22Ti ΣTM = 0.78 0.40421(9) nm	195	0.39	0.56	Al3($Sc_{0.64}Ti_{0.36}$) $L1_2$ up to 6–8 μm	0.4054 nm 0.29%	Not determined -
3	Al–0.46Sc–0.39Ti ΣTM = 0.85 4.0430(15) nm	240	0.85	0.89	Al3($Sc_{0.53}Ti_{0.47}$) $L1_2$ up to 28 μm	0.4039 nm 0.1%	0.40180(5) nm 0.62%
4	Al–0.60Sc–0.71Ti ΣTM = 1.30 0.40448(12) nm	85	1.18	1.13 49	Al3($Sc_{0.47}Ti_{0.53}$) $L1_2$ up to 6 μm, Al3($Ti_{0.98}Sc_{0.02}$) $D0_{22}$ up to 300 μm	0.4031 nm 0.34% – –	Not determined –
5	Al−0.67Sc−0.33Zr ΣTM = 1.00 0.40447(12) nm	200	0.49	1.0	Al3($Sc_{0.50}Zr_{0.50}$) $L1_2$ up to 20 μm	0.40915 nm 1.15%	0.40870(7) nm 1.05%
6	Al−0.25Sc−0.11Hf ΣTM = 0.36 0.40462(9) nm	370	0.44	0.85	Aln($Sc_{0.54}Hf_{0.46}$) $L1_2$ up to 6 μm	0.4078 nm 0.79%	0.406(1) nm 0.34%
7	Al−0.29Sc−0.26Hf ΣTM = 0.55 0.40452(10) nm	260	0.90	1.38	Aln($Sc_{0.42}Hf_{0.58}$) $L1_2$ up to 20 μm	0.4071 nm 0.64%	0.40601(17) nm 0.37
8	Al−0.26Sc−0.52Hf ΣTM = 0.78 0.40475(4) nm	240	2.0	2.45	Al_n($Sc_{0.29}Hf_{0.71}$) $L1_2$ up to 40 μm Al_3($Hf_{0.83}Sc_{0.17}$) $D0_{22}$ up to 100 μm	0.4064 nm 0.41% – –	0.40628(4) nm 0.38%

of ΔT (overheating above the liquidus temperature), the ratio of TMs (Ti, Zr, Hf) to Sc in alloys and aluminides, the calculated and experimental parameter of their lattices, and the absolute mismatch with α-Al are also given [23]. Diffraction studies were performed using a Shimadzu XRD-7000 instrument, Cu-K_α-radiation, graphite monochromator. The accumulation of data during 1.8 s in increments of 0.03° in the range of 20°–80°.

The Al–Sc–Ti system has a hypereutectic composition: the content of scandium and titanium varies from 0.46 to 0.60 at% and from 0.07 to 0.71 at%, respectively. The melting of the first three alloys was carried out at 930 °C, the fourth was melted at 900 °C. The Al–Sc–Zr alloy, having a hypereutectic composition of Al-0.67Sc-0.33Zr (at%), was melted at 1000 °C. In the Al–Sc–Hf system containing Sc from 0.25 to 0.29 at%, the Hf content varied almost fivefold from 0.11 to 0.52 at%. The melting temperature of the first and second alloys was 1100 °C, and 1170 °C for the third, with all the alloys (except the first) have a hypereutectic composition.

The X-ray phase composition for all experimental alloys showed that, along with α-Al, there is a phase with the $L1_2$ structural type. Figure 1 shows an example of a diffractogram for an Al-0.26Sc-0.52Hf alloy (alloy 8), where the lines of the Al_3Sc ($L1_2$) structural type are additionally marked with strokes. The experimental data of the α-Al lattice parameters and aluminides with the Al_3Sc structural type are shown in Table 1. For the 2 and 4 alloys, the diffraction pattern is not described by the Al3Sc structural type, there are additional reflections that could not be identified due to the low concentration of the precipitated phase as well as the low intensity of its reflexes.

3 Results and Discussion

3.1 Al–Sc–Ti System

In the Al–Sc–Ti alloys, overheated by 195–240 K above the liquidus temperature, metastable aluminides with a cubic lattice were formed. Their distribution, size and morphology are shown in Fig. 2.

In the first two alloys, aluminides have a cubic morphology. In the alloy Al-0.60Sc-0.07Ti (at%) cubic aluminides distribution is uniform, although in some places clusters are formed, the maximum size of aluminides does not exceed 3–4 μm. In the alloy Al-0.56Sc-0.22Ti (at%) the size of the aluminides is twice as large (the maximum size is 6–8 μm), the distribution is uneven. In the third alloy Al-0.46Sc-0.39Ti (at%) overheated by 240 K, cruciform aluminides

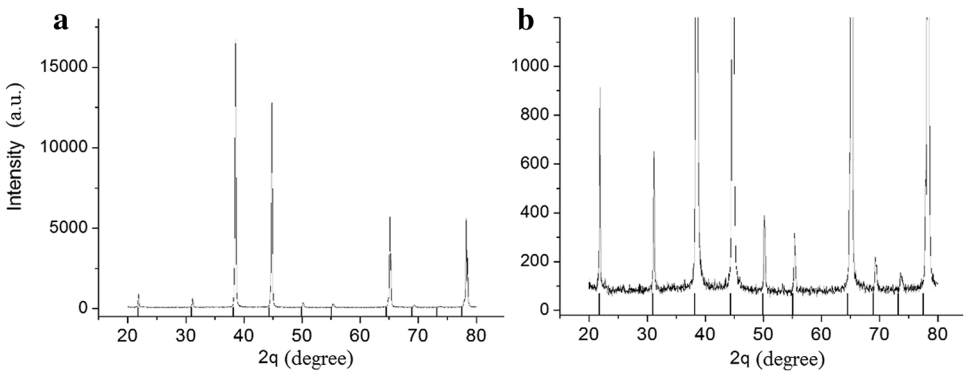

Fig. 1 Diffraction pattern of the Al-0.26Sc-0.52Hf alloy: **a** the aluminum lines are visible; **b** the lines of the Al_3Sc structural type are marked with strokes

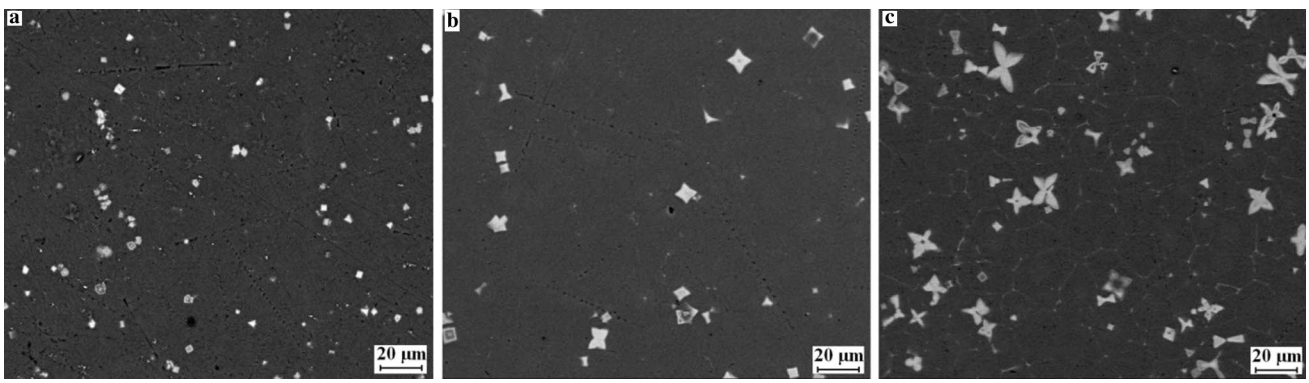

Fig. 2 Metastable aluminides in Al–Sc–Ti alloys: **a** Al-0.60Sc-0.07Ti (at%); **b** Al-0.56Sc-0.22% Ti (at%); **c** Al-0.46Sc-0.39Ti (at%)

with sizes up to 28 μm prevail, their growth forms are similar to scandium aluminides in the Al−1.2Sc (at%) master alloy [11]. Cubic aluminides are much smaller, their dimensions do not exceed 5 μm. The grain structure of the alloy is clearly manifested, the average grain size is 17 μm, thin eutectic veins are visible along the boundaries.

In alloys crystallizing at almost the same temperature and time intervals the maximum size and number of primary aluminides is determined by the sum of TMs. The higher it is in the alloy, the larger the aluminides grow. In the process of studying the influence of the cooling rate on the morphology of the primary Al_3Sc particles, Hyde et al. [24] showed that the cubic morphology appears to be a common feature of the primary $L1_2$ Al_3(TM) aluminides. However, at the slow cooling rate (1 K/s) of Al–Sc melts, clusters of homogeneous (solid) cubic aluminides are formed, and at cooling rates above 100 K/s they appear to have a cellular, or dendritic, substructure [24]. The formation of multilayer aluminide particles, as well as protrusions at growth points on the faces of cubic crystals at the slow cooling rates of the Al-Sc and Al–Sc–Ti melts were showed earlier [25, 26]. Under the cooling conditions studied in the present work, cubic aluminides having different structures (homogeneous, multilayered and with a cellular substructure) were formed. Examples of homogeneous sharply cubic $Al_3(Sc_{0.64}Ti_{0.36})$ and $Al_3(Sc_{0.53}Ti_{0.47})$ aluminides in the Al-0.56Sc-0.22Ti (at%) and Al-0.46Sc-0.39Ti (at%) alloys are shown in Fig. 3a–d. The linear scanning of the aluminides and the adjacent α-Al phase clearly showed almost constant intensity levels of analytical signals corresponding to Sc and Ti in aluminides. The levels of Sc and Ti signals are proportional to their contents, obtained from EDX point analysis. A gradual decrease in the signal intensity from Sc and Ti to the levels, corresponding to the alloy matrix, occurs at distances 1–1.5 μm on each side of the aluminide.

The composition of the Al-0.30Sc-0.12Ti (at%) alloy (Ti/Sc = 0.40) is studied in detail in [27], is close to the Al-0.56Sc-0.22Ti (at%) alloy (Ti/Sc = 0.39) obtained in the present work. The modifying ability of primary $L1_2$ Al_3(Sc,Ti) aluminides in a ternary alloy was compared with $L1_2$ Al_3Sc aluminides in a binary Al-0.42Sc (at%) alloy. Melts overheated by 100 K were poured into a wedge-shaped copper mold providing cooling rates from 100 to 1000 K/s. In the binary alloy (at the cooling rate of ≥ 100 K/s), the micron-size Al_3Sc particles had a sharply cubic morphology and formed clusters along the grain boundaries. Comparing the number of Al_3Sc particles detected at the grain boundaries with the particles at the grain center, the authors estimated the nucleation efficiency as one particle of 50. In a ternary alloy at the same cooling rate, the $L1_2$ Al_3(Sc,Ti) particles had rounded corners and sometimes spherical shape. Each particle nucleated a grain, i.e. the efficiency of nucleation

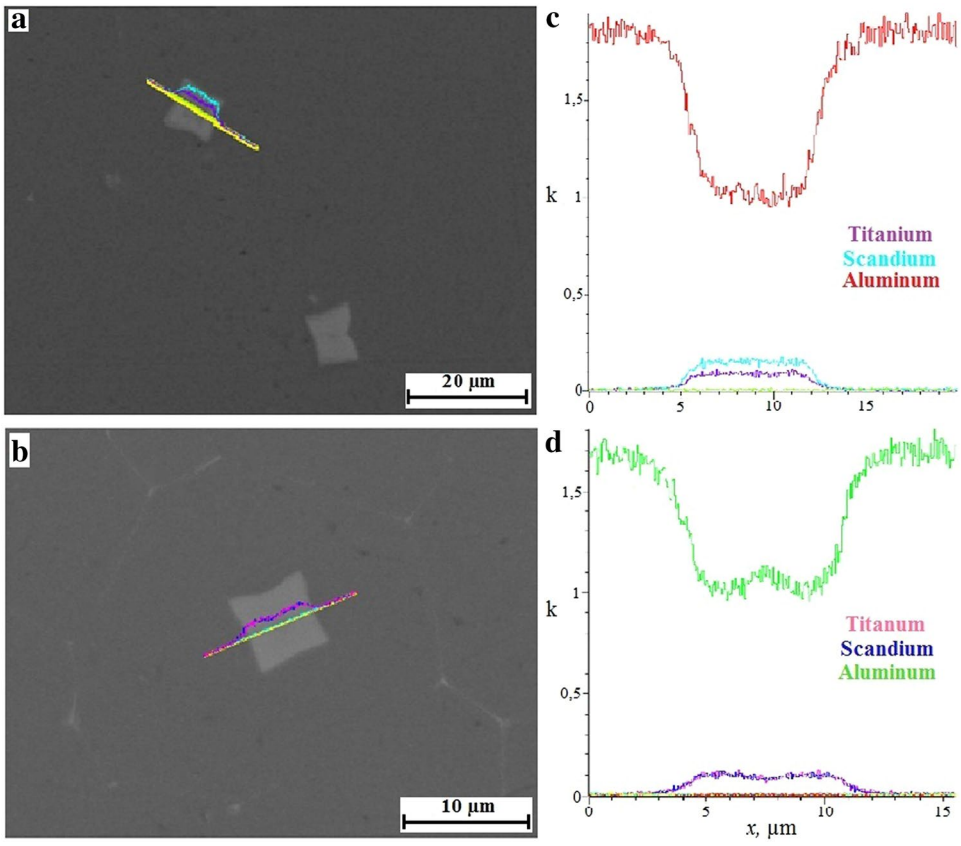

Fig. 3 Cross sections of cubic particles in Al-0.56Sc-0.22Ti (at%) and Al-0.46Sc-0.39Ti (at%) alloys: **a**, **b** $Al_3(Sc_{0.64}Ti_{0.36})$ and $Al_3(Sc_{0.53}Ti_{0.47})$ aluminides and their scanning lines, respectively; **c**, **d** analytical signals corresponding to Al, Sc and Ti

was 100%. The average composition of the primary particles observed in the ternary alloy corresponded to the $Al_3(Ti_{0.67}Sc_{0.33})$ composition and was out of keeping with the alloy composition: Ti/Sc = 2.03 in the aluminide and 0.40 in the alloy. The authors explained this by the fact that the presence of scandium stabilizes the cubic structure of the evolved metastable Al_3Ti aluminides, usually formed only at cooling rates of more than 104 K/s. As a result, aluminides of titanium are formed, with titanium is partially replaced by scandium.

As distinct from the first three master alloys (see Table 1), the Al-0.60Sc-0.71Ti (at%) alloy was melted with a small (~85°) overheating over the liquidus temperature.

(see Table 1). Moreover, the titanium content in the alloy exceeded the scandium content. As a result, $L1_2$ and $D0_{22}$ aluminides, with cubic and tetragonal lattices respectively, were formed in the alloy (Fig. 4). There are a large number of small (≤6 µm) mainly cubic $Al_3(Sc_{0\cdot47}Ti_{0.53})$ aluminides and long (up to 300 µm) needles consisting of stable $Al_3(Ti_{0.98}Sc_{0.02})$ aluminides, with titanium are slightly replaced by scandium. In this alloy, in addition to homogeneous cubic aluminides, multilayer particles are observed.

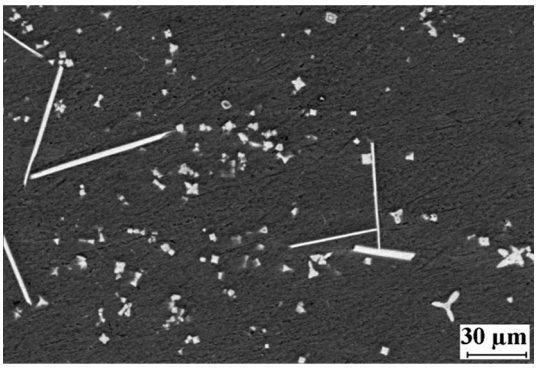

Fig. 4 Growth forms of both $L1_2$ and $D0_{22}$ aluminides in the Al–0.60Sc–0.71Ti (at%) alloy

According to the EDX analysis, scandium in the Al–Sc–Ti alloys is mainly included in the composition of aluminides. Scandium content varies from 0.19 to 0.36 at%, Sc is dissolved in the matrix and is a part of the fine eutectic formations. The higher the titanium content in the alloy, the larger the part of scandium replaced by titanium in the aluminide. Thus, with a Ti content increase by one order of magnitude (from 0.07 to 0.71 at%), its content in aluminides increases 4.4 times (from 0.12 to 0.53) (see Table 1).

4 Al–Sc–Zr System

The Al-0.67Sc-0.33Zr at% alloy having hypereutectic scandium and hyperperitectic titanium composition, was overheated by ~200 K above the liquidus temperature. The alloy is characterized by a nonuniform distribution of aluminide clusters having different growth forms: cubic, cruciform and dendritic morphology (Fig. 5). The size of cubic aluminides is up to 5 µm, cruciform - up to 14 µm and dendritic—up to 35 µm.

The distribution and morphology of the cruciform $Al_3(Sc_{0.50}Zr_{0.50})$ aluminides are similar to the Al-0.46Sc-0.39Ti (at%) alloy, however, their average linear size is about a half the size of $Al_3(Sc_{0.53}Ti_{0.47})$ aluminides. The fraction of zirconium in aluminides is ~0.50, although the Zr content in the alloy is a half the Sc (Sc/Zr = 2). A similar value of the titanium fraction in the $Al_3(Sc_{0.53}Ti_{0.47})$ aluminide is achieved at almost equal Sc and Ti content (Sc/Ti = 1.18) in the Al-0.46Sc-0.39Ti (at%) alloy. The greater activity of Zr, compared with Ti, in the process of aluminides formation during crystallization of the alloy can be explained by the difference of diffusion coefficients: their values are at 400 °C 1.20×10^{-20} and 7.39×10^{-22} $m^2\ s^{-1}$ [28], respectively. The difference by one order of magnitude is maintained even at the solidification temperature of pure aluminum.

Aluminides have mostly homogeneous structure. The distribution of Sc and Zr over the cross-section (6 µm) of the $Al_3(Sc_{0.50}Zr_{0.50})$ aluminide in the Al-0.67Sc-0.33 Zr

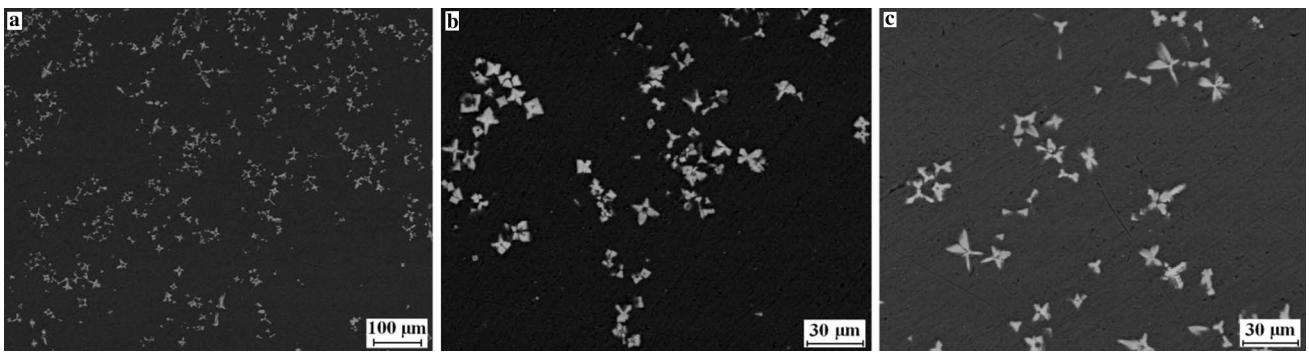

Fig. 5 Metastable aluminides $Al_3(Sc_{0.50}Zr_{0.50})$ in the Al-0.67Sc-0.33Zr (at%) alloy: **a** distribution **b**, **c** growth forms

(at%) alloy are shown in Fig. 6a, b. In the linear scan of the $Al_3(Sc_{0.50}Zr_{0.50})$ and the adjacent α-Al phase, as well as in Al–Sc–Ti alloys, constant levels of the intensity of the analytical signals corresponding to Sc and Zr in aluminides and their gradual decrease to the level of signals in the matrix are observed. Signal levels corresponding Sc and Zr are proportional to the Sc and Zr contents obtained from EDX point analysis.

The Al-0.6Sc-0.3Zr (at%) alloy with the same TMs ratio (Sc/Zr = 2) as in our alloy was investigated in [29]. The alloy was prepared in a vacuum furnace at the temperature of 720 ± 5 °C with an annealing for 30 min and poured into a wedge-shaped copper mold. At a cooling rate of ~ 600 K/s, the primary extracted particles had a sharply cubic and cubic morphology, and a cruciform at ~ 100 deg/s, the composition of the primary aluminides is not determined.

The formation of primary $L1_2$ aluminides in a ternary Al-0.1Sc-0.1Zr (at%) dilute alloy was also investigated in [30]. Alloys [ternary and binary Al-0.1Sc, Al-0.1Zr (at%)] were prepared in an electric-arc furnace with a non-consumable tungsten electrode in an argon atmosphere (remelting at least 10 times). The ingots (7 g) were crystallized on a water-cooled copper cathode. The macrostructure with coarse columnar millimeter grains, typical for cast binary alloys of this composition, in a ternary alloy became equiaxed with a grain size of 50 µm. It was a manifestation of the synergistic effect with the combined influence of Sc + Zr. Primary aluminides (from 3 to 5 µm) had a petal morphology characteristic for $L1_2$ structure of metastable Al_3Zr or equilibrium Al_3Sc aluminides. In the $Al_3(Zr_{0.75}Sc_{0.25})$ aluminide, the amount of zirconium was three times greater than the amount of scandium. It does not correspond to the composition of the alloy with ratio of Zr/Sc = 1.

5 Al–Sc–Hf System

Metastable $L1_2$ aluminides were formed during the crystallization of the Al-0.25Sc-0.11Hf (at%), Al-0.29Sc-0.26Hf (at%) and Al-0.26Sc-0.52Hf (at%) alloys, obtained by overheating the melts above the liquidus temperarure by 370, 260 and 240 K, respectively. The high overheating of the melts determines the variety of growth forms. Multilayered and homogeneous aluminides form $Al_n(Sc_xHf_{1-x})$ solid solutions, with n varies from 4 to 26. The higher the overheating, the greater the value of n. The content of hafnium in aluminides increased from 0.46 to 0.71 proportionally to the increase in hafnium content in alloys. The alloys, as shown in Fig. 6, have a characteristic cellular microstructure [31]. The dimensions of the cells and aluminides decrease with increasing of melt overheating.

In the Al-0.25Sc-0.11Hf (at%) alloy, overheated by 370 K, the cell sizes coincide with the grain size of 10–15 µm. The $Al_n(Sc_{0.54}Hf_{0.46})$ aluminides, formed in this alloy, have a cubic morphology, are located in the center of grains, and their maximum size does not exceed 6 µm. $Al_n(Sc_{0.42}Hf_{0.58})$ aluminides were formed in the Al-0.29Sc-0.26Hf (at%) alloy, overheated by 260 K. The average size of the aluminides is 4–5 times larger than in the first alloy. The aluminides had a cubic and cruciform structure with particle size ≤ 20 µm and are in the center of the grains. The grain size was from 10 to 30 µm. The cross-sections of a layered cubic particle (4.5 µm in size) in the first alloy and a homogeneous cruciform particle (20 µm in size) in the second alloy are shown in Fig. 7a–d. As in Al–Sc–Ti and Al–Sc–Zr alloys, constant intensity levels of analytical signals received from Sc and Hf in aluminides are observed. Both aluminides are surrounded by visible "shells"—layers of different sizes (2 and 4 µm), in which the intensity of signals is gradually reduced from Sc and Hf to a matrix level.

In the Al-0.26Sc-0.52Hf (at%) alloy (with a high hafnium content and overheating by 240 K), $Al_n(Sc_{0.29}Hf_{0.71})$

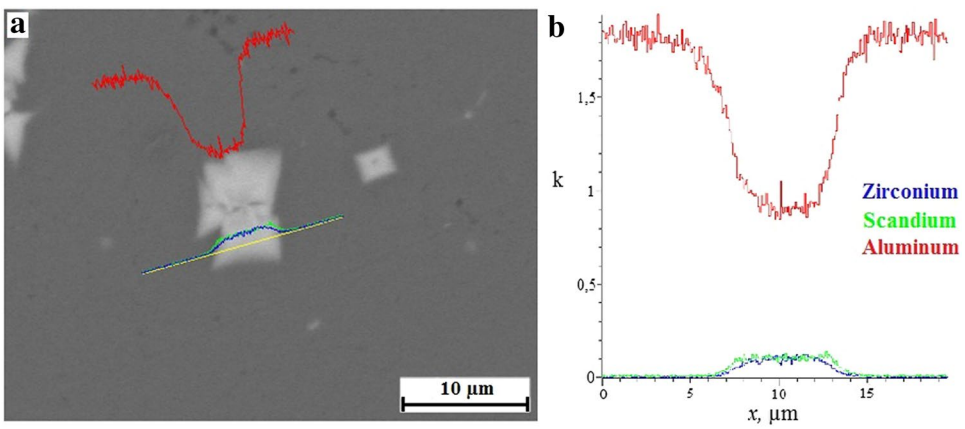

Fig. 6 Cross section of the $Al_3(Sc_{0.50}Zr_{0.50})$ particle: **a** the particle and the scan line **b** analytical signals corresponding to Al, Sc and Zr

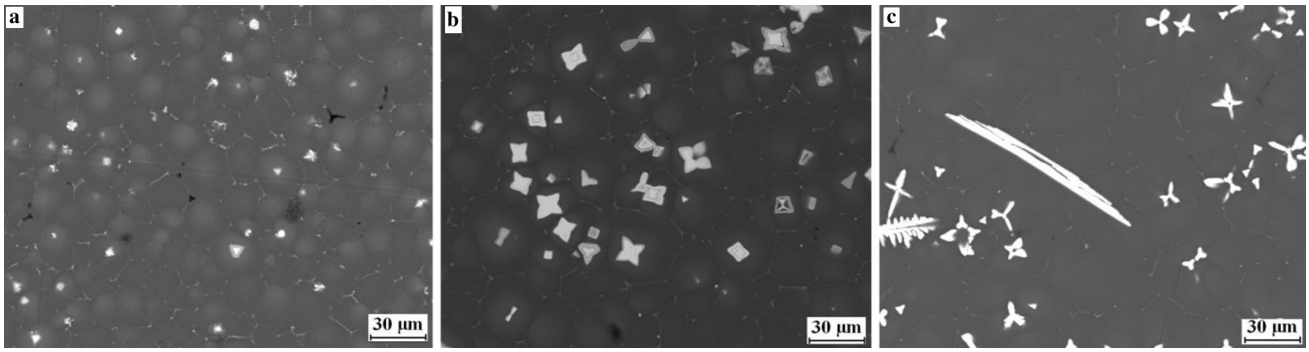

Fig. 7 Microstructure of the alloys: **a** Al-0.25Sc-0.11Hf (at%); **b** Al-0.29Sc-0.26Hf (at%); and **c** Al-0.26Sc-0.52Hf (at%)

aluminides having a cubic lattice had mainly a cross-shaped morphology. Large clusters of dendritic aluminides up to 40 μm are also observed. In addition, separate $Al_3(Hf_{0.83}Sc_{0.17})$ aluminides having a tetragonal lattice (plates and needles up to 100 μm, see Fig. 8c) were formed, with scandium replaces up to 17% of hafnium. The alloy grain was of different size with the dendritic structure of the α-phase. Thin veins of the eutectic containing 0.33 at% Sc were formed on the grain boundaries. The solubility of hafnium in the center of the α-Al dendrites reaches 0.48%, in interdendritic spaces the composition is 100% Al.

The ratio of Hf to Sc in aluminides was lower than in alloys, with the difference increase almost twofold with an increase in the melt overheating to 370 K. This is explained by the tendency of hafnium to microsegregation under non-equilibrium conditions of alloys crystallization. The content of hafnium decreases from the center of the α-Al dendritic cells to their boundaries. The higher the overheating of the melt is, the greater the supersaturation of α-Al by dissolved element is. According to the EDX analysis of the studied alloys, the content of hafnium in the center of the α-Al dendritic cells exceeds their volume contents: 1.5 times in

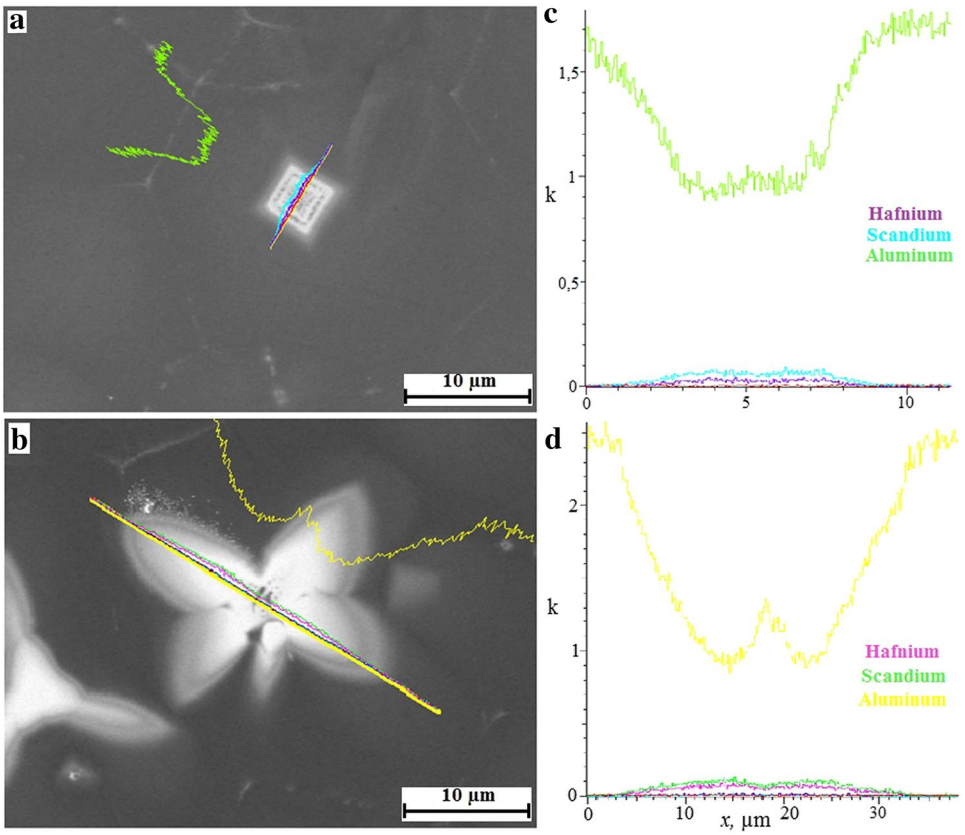

Fig. 8 Cross sections of aluminide particles in the alloys Al-0.25Sc-0.11Hf (at%) and Al-0.29Sc-0.26Hf (at%): **a**, **b** $Al_n(Sc_{0.54}Hf_{0.46})$ and $Al_n(Sc_{0.42}Hf_{0.58})$ aluminides and their scanning lines, respectively; **c**, **d** analytical signals corresponding to Al, Sc and Hf

the Al-0.29Sc-0.26Hf (at%) alloy and 3.3 times in the Al-0.25Sc-0.11Hf (at%) alloy.

The influence of small additions of Sc and Zr on the structure of Al-Hf cast alloys was studied in [29]. Alloys of different hafnium composition were prepared from high-purity aluminum and binary master alloys. The melts were mixed and poured at 760 °C into cylindrical shapes (Ø40 mm × 150 mm) mounted on a large copper cylinder (cooling rate was from 5 to 10 K/s), providing directional crystallization to reduce a porosity and a shrinkage. The authors showed that in order to prevent the formation of a double columnar structure in the cast alloy, the Hf content should be below 0.11 at% Hf (< 0.7 wt%). With the addition of scandium, the equilibrium grain structure was formed in a cast Al-0.12Sc-0.03Hf (at%) alloy. A dense and homogeneous distribution of secondary aluminides (precipitates) is achieved in the aging process of the alloy. It leads to an increase in the strength of the alloy and to an increase the recrystallization resistance.

6 Lattices Parameter Determination

The solubility limits of transition metals (Ti, Zr, Hf, etc.) in the lattice of scandium aluminide without a violation of $L1_2$ cubic structure and corresponding changes in the lattice parameters of ternary aluminides were studied in [32]. Alloys corresponding to the composition of the aluminides were prepared according to the procedure [30] described above. The ingots were homogenized for 2 h in a vacuum (10^{-4} Pa) at 1200 °C. The limiting solubility of Ti, Zr, Hf in scandium aluminide without changing the structural type of the lattice reached 12.5 at%. In that way, $D0_{22}$ or $D0_{23}$ aluminides were formed in addition to $L1_2$ $Al_3(Sc_{0.5}Ti_{0.5})$, $Al_3(Sc_{0.5}Zr_{0.5})$ and $Al_3(Sc_{0.5}Hf_{0.5})$ aluminides. With a further increase in the addition of Ti and Hf, the resulting aluminides had only tetragonal lattices. In contrast to Ti and Hf, when Sc was substituted with zirconium, even the $Al_3(Sc_{0.25}Zr_{0.75})$ aluminides still retained two lattice types. These results coincide with the data of works [3] and [4], according to which the metastable $L1_2$ Al_3Zr phase is formed more easily than the $L1_2$ Al_3Ti phase during the high-speed crystallization of Al-Ti and Al-Zr melts from temperatures of 1100–1200 °C. According to [32], there is a linear relationship between the lattice parameter of the forming aluminide and the concentration of transition metals (Ti, Zr or Hf). The lattice parameter decreases with increase in the concentration of Ti, Zr and Hf. The change in the lattice parameter upon addition of Ti is much greater than when Zr or Hf are added.

Using the data on the lattice parameters of $Al_3(Sc,TM)$ aluminides [32] and the calculated values of the lattice parameter of Al_3TM [13], where the TM is Ti, Zr or Hf, we estimated the lattice parameters of the aluminide in the experimental master alloys and their mismatch to the.

α-Al (see Table 1). All mismatches don't exceed 1,15%, i.e. when modifying aluminum alloys with these master alloys, a synergistic effect of two TMs for grain refinement should appear. It is assumed that further experiments will be conducted to detect this effect at a minimum cooling rate (1 K/s).

7 Conclusions

Al–Sc–Ti, Al–Sc–Zr, Al–Sc–Hf master alloys containing metastable $L1_2$ aluminides were synthesized.

Metastable aluminides are formed by rapid crystallization of overheated (by 100–370 K above the liquidus temperature) Al–Sc–TM melts. The ratio of Sc to Ti, Zr or Hf in the resulting aluminides is proportional to that in alloys. Forming aluminides have both a homogeneous and a layered substructure.

The variety of growth forms and substructures of aluminides can be explained by a combination of a number of factors: the magnitude of melt overheating, the difference in the diffusion coefficients of transition metals, and also their local concentration in the corresponding growth zones.

Estimation of the lattice parameters of the experimental master alloys showed, that mismatches with the α-Al lattice are about 1%, that should significantly increase their modifying ability.

Acknowledgments The work was carried out according to the state assignment for IMET UB RAS. The results were obtained using the equipment of the Ural-M Center for Collective Use.

References

1. Z. Li, H. Jiang, Y. Wang, D. Zhang, D. Yan, L. Rong, Effect of minor Sc addition on microstructure and stress corrosion cracking behavior of medium strength Al–Zn–Mg alloy. J. Mater. Sci. Technol. **34**(7), 1172–1179 (2018)
2. J. Zhang, H. Wang, D. Yi, B. Wang, H. Wang, Comparative study of Sc and Er addition on microstructure, mechanical properties, and electrical conductivity of Al-0.2Zr-based alloy cables. Mater. Charact. **145**, 126–134 (2018)
3. S.H. Wu, P. Zhang, D. Shao, P.M. Cheng, J. Kuang, K. Wu, J.Y. Zhang, G. Liu, J. Sun, Show more grain size-dependent Sc microalloying effect on the yield strength-pitting corrosion correlation in Al–Cu alloys. Mater. Sci. Eng. A **721**(4), 200–214 (2018)
4. N. Belov, E. Naumova, T. Akopyan, Effect of 0.3% Sc on microstructure, phase composition and hardening of Al–Ca–Si eutectic alloys. Trans. Nonferrous Metals Soc. China **27**(4), 741–746 (2017)
5. D. Erdeniz, W. Nasim, J. Malik, A.R. Yost, S. Park, A. De Luca, N.Q. Vo, I. Karaman, B. Mansoor, D.N. Seidman, D.C. Dunand, Effect of vanadium micro-alloying on the microstructural

evolution and creep behavior of Al–Er–Sc–Zr–Si alloys. Acta Mater. **124**, 501–512 (2017)
6. J.H. Li, M. Wiessner, M. Albu, S. Wurster, B. Sartory, F. Hofer, P. Schumacher, Correlative characterization of primary Al3(Sc, Zr) phase in an Al–Zn–Mg based alloy. Mater. Charact. **102**, 62–70 (2015)
7. S. Saumitra, T.Z. Todorova, J.W. Zwanziger, Temperature dependent lattice misfit and coherency of Al3X (X = Sc, Zr, Ti and Nb) particles in an Al matrix. Acta Mater. **89**, 109–115 (2015)
8. T. Dorin, M. Ramajayam, J. Lamb, T. Langan, Effect of Sc and Zr additions on the microstructure/strength of Al–Cu binary alloys. Mater. Sci. Eng. A **707**, 58–64 (2017)
9. H. Hallem, W. Lefebvre, B. Forbord, F. Danoix, K. Marthinsen, The formation of $Al_3(Sc_xZr_yHf_{1-x-y})$-dispersoids in aluminium alloys. Mater. Sci. Eng. A **421**, 154–160 (2006)
10. H. Hallem, B. Forbord, K. Marthinsen, An investigation of dilute Al–Hf and Al–Hf–Si alloys. Mater. Sci. Eng. A **387–389**, 940–943 (2004)
11. A.F. Norman, P.B. Prangnell, R.S. McEwen, The solidification behavior of dilute aluminium–scandium alloys. Acta Mater. **46**(16), 5715–5732 (1998)
12. S. Srinivasan, P.B. Desch, R.B. Schwarz, Metastable phases in the Al_3X (X = Ti, Zr, and Hf) intermetallic system. Scripta Metall. Mater. **25**(11), 2513–2516 (1991)
13. I.G. Brodova, I.V. Polents, V.O. Esin, E.M. Lobov, On the formation of the cast structure of supercooled Al–Ti alloys. Phys. Metals Metall. **73**(1), 63–67 (1992)
14. P. Malek, M. Janecek, B. Smola, P. Bartuska, J. Plestil, Structure and properties of rapidly solidified Al–Zr–Ti alloys. J. Mater. Sci. **35**, 2625–2633 (2000)
15. A.F. Norman, P. Tsakiropoulos, Rapid solidification of Al–Hf alloys—solidification, microstructures and decomposition of solid-solutions. Int. J. Rapid Solid **6**(3–4), 185–213 (1991)
16. E.A. Popova, A.B. Shubin, P.V. Kotenkov, E.A. Pastukhov, L.E. Bodrova, O.M. Fedorova, Al–Ti–Zr master alloys: structure formation. Russ. Metall. (Metally) **2012**(5), 357–361 (2012)
17. E.A. Popova, P.V. Kotenkov, E.A. Pastukhov, A.B. Shubin, Master alloys Al–Sc–Zr, Al–Sc–Ti, and Al–Ti–Zr: their manufacture, composition, and structure. Russ. Metall. (Metally) **2013**(8), 590–594 (2013)
18. E.A. Popova, A.B. Shubin, P.V. Kotenkov, L.E. Bodrova, A.V. Dolmatov, E.A. Pastukhov, N.A. Vatolin, Al–Sc–Zr Master alloy and estimation of its modifying capacity. Russ. Metall. (Metally) **2011**(8), 715–718 (2011)
19. E.A. Popova, P.V. Kotenkov, E.A. Pastukhov, Synergetic effect in modifying with master alloys having an aluminide cubic structure. Russ. Metall. (Metally) **2016**(2), 189–193 (2016)
20. J.L. Murray, The Al–Sc (Aluminum–Scandium) system. J. Phase. Equil. **19**(4), 380–384 (1998)
21. K.E. Knipling, D.C. Dunand, D.N. Seidman, Nucleation and precipitation strengthening in dilute Al–Ti and Al–Zr alloys. Metall. Mater. Trans. A **38**, 2552–2563 (2007)
22. J.L. Murray, A.J. McAlister, D.J. Kahan, The Al–Hf (Aluminum–Hafnium) system. J. Phase. Equil. **19**(4), 376–379 (1998)
23. G. Ghosh, M. Asta, First-principles calculation of structural energetics of Al–TM (TM = Ti, Zr, Hf) intermetallics. Acta Mater. **53**, 3225–3252 (2005)
24. K.B. Hyde, A.F. Norman, P.B. Prangnell, The effect of cooling rate on the morphology of primary Al_3Sc intermetallic particles in Al–Sc alloys. Acta Mater. **49**, 1327–1337 (2001)
25. A.V. Shubin, E.A. Popova, KYu. Shunyev, E.A. Pastukhov, Slow crystallization Al–Sc alloys: growth of spherical intermetallic particles. Defect Diffus. Forum **326–328**, 75–80 (2012)
26. A.B. Shubin, E.A. Popova, P.V. Kotenkov, E.A. Pastukhov, Crystallization of Al–Sc–Ti alloys at low cooling rates: morphology of intermetallic particles. Melts **5**, 3–11 (2015). **(In Russian)**
27. K.B. Hyde, A.F. Norman, P.B. Prangnell, The effect of Ti on grain refinement in Al–Sc alloys. Mater. Sci. Forum **396–402**, 39–44 (2002)
28. S.I. Fujikawa, Solid state diffusion in light metals. J. Jpn. Inst. Light Metals **46**(4), 202–215 (1996)
29. X.U. Cong, D.U. Rou, X.J. Wang, S. Hanada, H. Yamagata, W.H. Wang, C.L. Ma, Effect of cooling rate on morphology of primary particles in Al−Sc−Zr master alloy. Trans. Nonferrous Met. Soc. China **24**, 2420–2426 (2014)
30. K.E. Knipling, R.A. Karnesky, C.P. Lee, D.C. Dunand, D.N. Seidman, Precipitation evolution in Al–0.1Sc, Al–0.1Zr and Al–0.1Sc–0.1Zr (at.%) alloys during isochronal aging. Acta Mater. **58**, 5184–5195 (2010)
31. H. Hallem, B. Forbord, K. Marthinsen, An investigation of cast structures in Al–Hf– (Sc)–(Zr) alloys and their subsequent effect on recrystallisation resistance after cold rolling. Mater. Forum **28**, 240–245 (2004)
32. Y. Harada, D.C. Dunand, Microstructure of Al_3Sc with ternary transition-metal additions. Mater. Sci. Eng. A **329–331**, 686–695 (2002)